FEBS Letters 588 (2014) 1802–1807

FEBS Letters

journal homepage: www.FEBSLetters.org

On the substrate- and stereospecificity of the plant carotenoid cleavage dioxygenase 7

Mark Bruno [a,1], Manuel Hofmann [a,1], Martina Vermathen [b], Adrian Alder [a], Peter Beyer [a], Salim Al-Babili [a,c,*]

[a] Albert-Ludwigs University of Freiburg, Faculty of Biology, Schaenzlestr. 1, D-79104 Freiburg, Germany
[b] Department of Chemistry and Biochemistry, University of Bern, 3012 Bern, Switzerland
[c] Center for Desert Agriculture, BESE Division, King Abdullah University of Science and Technology (KAUST), 23955-6900 Thuwal, Saudi Arabia

ARTICLE INFO

Article history:
Received 11 February 2014
Revised 17 March 2014
Accepted 19 March 2014
Available online 28 March 2014

Edited by Julian Schroeder

Keywords:
Apocarotenoid
Carlactone
Carotenoid
Carotenoid cleavage dioxygenase
Strigolactone

ABSTRACT

Strigolactones are phytohormones synthesized from carotenoids via a stereospecific pathway involving the carotenoid cleavage dioxygenases 7 (CCD7) and 8. CCD7 cleaves 9-*cis*-β-carotene to form a supposedly 9-*cis*-configured β-apo-10′-carotenal. CCD8 converts this intermediate through a combination of yet undetermined reactions into the strigolactone-like compound carlactone. Here, we investigated the substrate and stereo-specificity of the Arabidopsis and pea CCD7 and determined the stereo-configuration of the β-apo-10′-carotenal intermediate by using Nuclear Magnetic Resonance Spectroscopy. Our data unequivocally demonstrate the 9-*cis*-configuration of the intermediate. Both CCD7s cleave different 9-*cis*-carotenoids, yielding hydroxylated 9-*cis*-apo-10′-carotenals that may lead to hydroxylated carlactones, but show highest affinity for 9-*cis*-β-carotene.

1. Introduction

Strigolactones (SLs) are a novel class of plant hormones that determine various aspects of plant development [1–6], including shoot branching [7,8], root architecture [9–11], senescence [12] and cambium secondary growth [13]. Released by plants into the rhizosphere, SLs also induce hyphal branching of symbiotic fungi [14], a prerequisite for establishing mycorrhizal symbiosis that provides the plant hosts with water and minerals. SLs also trigger seed germination of obligate root parasitic plants, such as *Striga* and *Orobanche* species [1–3].

SLs belong to the apocarotenoids [15–18], a group of carotenoid-derived, physiologically important compounds that includes retinoids, the phytohormone abscisic acid and the fungal pheromone trisporic acid [19]. The precursors of SLs, the carotenoids, are isoprenoid pigments with an extended conjugated double bond system synthesized by all photosynthetic organisms and many heterotrophic bacteria and fungi [20–23]. Plants accumulate several carotenoids that derive from the colorless carotene phytoene. Desaturation and isomerization reactions lead to lycopene, the red linear precursor of the bicyclic β-and ε-carotene. Hydroxylation of the β- and ε-ring of β-carotene and of the ε-ionone rings of ε-carotene give rise to zeaxanthin and lutein, respectively. Zeaxanthin can be epoxydated to yield violaxanthin the precursor of neoxanthin that carries an epoxydated β-ionone ring on the one end and an allen system on the other. Plant carotenoids also differ in their stereo-configuration and occur all-*trans* configured as well as in different *cis*-isomeric forms like 9-*cis*-violaxanthin and 9-*cis*-β-carotene, the precursors of abscisic acid and SLs, respectively [15,16,24]. Like with other apocarotenoids, the synthesis of these hormones is initiated by oxidative cleavage of double bonds in carotenoid backbones, a reaction that is generally catalyzed by carotenoid cleavage oxygenases.

Plant carotenoid cleavage oxygenases are classified into nine-*cis*-epoxy-carotenoid-dioxygenases that cleave 9-*cis*-violaxanthin and 9′-*cis*-neoxanthin to yield xanthoxin the precursor of ABA, and carotenoid cleavage dioxygenases (CCDs), a general term applied for all other members of this plant enzyme family [15–17]. Plant CCDs are divided into 4 groups, CCD1, CCD4, CCD7 and CCD8, differing in their substrate specificities and cleavage sites [15–17]. CCD1 enzymes are characterized by wide substrate and cleavage-site specificity [15,16,25], cleaving cyclic and acyclic

* Corresponding author at: Center for Desert Agriculture, BESE Division, King Abdullah University of Science and Technology (KAUST), 23955-6900 Thuwal, Saudi Arabia.

E-mail address: salim.babili@kaust.edu.sa (S. Al-Babili).

[1] These authors contributed equally to this work.

http://dx.doi.org/10.1016/j.febslet.2014.03.041
0014-5793/

all-*trans*-carotenoids [17], as well as apocarotenoids, like β-apo-8′-carotenal [26,27], β-apo-10′-carotenal and apolycopenals [28]. This activity leads to various volatiles like β-ionone, 6-methyl-5 hepten-2-one (MHO; C8) [27] and geranial [28], and indicates a function in scavenging destructed carotenoids [29]. CCD4 enzymes from different plants produce β-ionone by cleaving β-carotene or β-apo-8′-carotenal at the C9–C10 double bond [30,31], and studies on the Arabidopsis CCD4 suggested its role as a negative regulator of the β-carotene level in seeds [32,33]. Similarly, decreasing the activity of CCD enzymes lead to an enhancement in carotenoid content of chrysanthemum flowers [34], potato tubers [35] and peach fruits [36]. However, it was recently reported that CCD4 enzymes contributes to the deep color of *Citrus* fruit peels by cleaving the 7′,8′ double bond in β-carotene, β-cryptoxanthin and zeaxanthin, leading to the pigments β-apo-8′-carotenal and 3-OH-β-apo-8′-carotenal (β-citraurin) [37,38].

CCD7 and CCD8 are involved in SLs biosynthesis [7,8]. Expression of CCD7 from Arabidopsis and tomato in carotenoid accumulating *Escherichia coli* strains suggested the cleavage at the 9,10 or 9′,10′ site, leading to C_{13} volatiles, e.g. β-ionone, and C_{27} apocarotenals such as β-apo-10′-carotenal [39,40], which is converted upon co-expression of the Arabidopsis CCD8 into β-apo-13-carotenone [40]. Considering that the *E. coli* strains used mainly accumulate all-*trans*-configured carotenoids, these results indicated that SLs are synthesized via the intermediate β-apo-13-carotenone produced by CCD7 and CCD8 from all-*trans*-β-carotene. However, a recent in vitro study suggested a new path to SLs via carlactone [24], a SLs-like compound that has been very recently also identified *in planta* [41]. This pathway starts with the D27-catalyzed isomerization of all-*trans*- into 9-*cis*-β-carotene that is cleaved by CCD7 to yield β-ionone and 9-*cis*-β-apo-10′-carotenal used by CCD8 to form carlactone, supposedly by catalyzing a combination of different reactions [24]. The 9-*cis* identity of the apocarotenal produced by CCD7 was determined by HPLC-comparison with a synthetic all-*trans*-β-apocarotenal and to a supposedly 9-*cis*-configured β-apo-10′-carotenal produced by a CCD1 from 9-*cis*-β-carotene [42].

The stereo-configuration of the β-apo-10′-carotenal produced by CCD7 determines the nature of the CCD8 product and is crucial for identifying and understanding the reactions leading to carlactone [24,43]. In addition, the cleavage of 9-*cis*-configured carotenoids other than 9-*cis*-β-carotene by CCD7 may lead to the formation of novel carlactone species, like 3-OH-carlactone, and, hence, to novel types of strigolactones. In this study, we unequivocally determined the configuration of the β-apo-10′-carotenal produced by the Arabidopsis CCD7, using NMR, and investigated the substrate specificity of the Arabidopsis and pea CCD7.

2. Materials and methods

2.1. Photometrical measurements

Substrates were quantified spectrophotometrically at their individual λ_{max} according to the extinction coefficients calculated from E1% as given by [44]. Protein contents were determined using a Biorad Bradford protein assay (BIO-RAD).

2.2. Isomerization and preparation of carotenoids

9-*cis*-β-carotene was purchased from Carotenature. Cryptoxanthin and zeaxanthin were kindly provided by the BASF (Ludwigshafen). Lutein and violaxanthin were isolated from spinach. For isomerization, carotenoids were dissolved in n-hexan or CH_2Cl_2, and a catalytic quantity of iodine solved in n-hexan was added. The Solution was exposed to a table lamp for 30 min. Lipophilic pigments were partitioned using water, petroleum ether/diethyl ether (1:4) and acetone, washed several times with water and dried. Isomers obtained were separated and collected by HPLC.

2.3. HPLC

For preparative isolation, we used a Waters separation system 2695 equipped with a photodiode array detector (model 2996) and a YMC-Pack C30-reversed phase column (250 × 10 mm i.d., 5 μm; YMC Europe, Schermbeck, Germany). The collected fractions were dried and resolved in CH_2Cl_2. Lutein, zeaxanthin and cryptoxanthin isomers were separated with the solvents B: MeOH/H_2O/TBME (60:12:12, v/v/v) and A: MeOH/TBME (50:50, v/v). The column was developed isocratically with 50% A at a flow-rate of 2.4 ml/min for 5 min, followed by a linear gradient to 80% A within 20 min, then to 100% A within 2 min. The final conditions were kept at a flow rate of 3 ml/min for 5.5 min. Violaxanthin isomers were separated with the solvents B: MeOH/H_2O/TBME (30:10:1, v/v/v) and A: MeOH/TBME (50:50, v/v). The column was developed isocratically with 65% A at a flow-rate of 2.4 ml/min for 8 min, followed by a linear gradient to 75% A within 8 min. The final conditions were kept for 6 min.

In vitro assays were analyzed using a YMC-Pack C30-reversed phase column (150 × 4.6 mm i.d., 5 μm; YMC Europe, Schermbeck, Germany) and the solvent B: MeOH/H2O/TBME (5:1:1, v/v/v) and A: MeOH/TBME (1:1, v/v). The column was developed at a flow-rate of 0.75 ml/min with a gradient from 100% B to 100% A within 20 min, maintaining these final conditions for 4 min.

2.4. In vitro assays

BL21(DE3) *E. coli* cells that contain the plasmid pGro7 were transformed with pThio-AtCCD7 and pThio-PsCCD7 expressing the thioredoxin-fusion of each enzyme [24]. Control cells were transformed with the void plasmid pBAD/THIO-TOPO®TA (Invitrogen). Crude lysates were obtained and prepared as described previously [43]. Standard in vitro assays were performed in a total volume of 200 μl containing the substrate at a 160 μM concentration and 50 μl of crude lysate of expressing *E. coli* cells. Crude lysates and assays were prepared and conducted according to [43]. The plasmid pThio-DAN2-AtNCED2 was used as a positive control in the 9-*cis*-violaxanthin assay (Supplementary Fig. 2) prepared like other assays. It was constructed by amplifying the AtNCED2 [45] cDNA from Arabidopsis total cDNA, using the *Phusion* High-Fidelity DNA Polymerase (Finnzymes) and the primers: AtNCED2for: 5′atggtttctcttcttacaatgccgatgag3′ and AtNCED2rev: 5′ ttataattgatcaacgagttcattcgaatcc 3′. The obtained fragment was ligated into pCR2.1 (Invitrogen) and subsequently inserted into pThio-DAN2, a derivative of pBAD®/Thio-TOPO® (Invitrogen).

2.5. Michaelis–Menten kinetics

2.5.1. In vitro assays for Michaelis–Menten

Kinetic measurements were performed in vitro like standard assays, however, with substrate concentrations ranging from 5 to 140 μM and 3.75 μg/μl total protein concentration. Assays were incubated for 5 min at 28 °C under shaking. Three technical replicates of each substrate concentration were performed. Assays were extracted according to [43], and extracts were dissolved in 40 μl $CHCl_3$ and analyzed by HPLC, using tocopherole acetate as internal standard. Total amounts of products were calculated based on calibration with synthetic all-*trans*-β-apo-10′-carotenal. Curve fitting was done, using the Michaelis–Menten equation, with the GraphPad Prism 6 software (GraphPad Software, La Jolla, USA).

2.6. Large scale in vitro assay and purification of 9-cis-β-apo-10′-carotenal

The assay was performed in a total volume of 100 ml. 8.28 ml of 1.45 mM CH_2Cl_2 solution of 9-*cis*-β-carotene was mixed with 10 ml of 0.8%, v/v ethanolic Triton X-100 (Sigma, Deisenhofen) solution, Sigma, Deisenhofen, Germany), dried and re-suspended in 25 ml H_2O. The micelles were mixed with 50 ml 2 × incubation buffer [43], and 25 ml of crude lysate was then added. After incubation for 6 h at 28 °C, lipophilic compounds were extracted according to [43], dried and dissolved in CH_2Cl_2. The extract was then separated by thin-layer silica reverse phase plates (RP-18; Merk, Darmstadt) developed in methanol/water (100:1, v/v), and 9-*cis*-β-apo-10′-carotenal was scraped off in dim daylight and eluted with CH_2Cl_2. For purification, we used two different HPLC systems. The first consisted of a YMC-Pack C30-reversed phase column (250 × 10 mm i.d., 5 μm; YMC Europe, Schermbeck, Germany) with the solvent B: MeOH/H_2O/TBME (60:12:12, v/v/v) and A: MeOH/TBME (50:50, v/v). The column was developed isocratically with 40% A at a flow-rate of 2.1 ml/min for 24 min, followed by switching to 100% A within 1 min and enhancing the flow-rate to 3 ml/min within 3 min. The second purification step was performed using a MN Nucleosil 100 C18-reversed phase column (250 × 4 mm i.d., 10 μm; Machery-Nagel, Düren, Germany). The column was developed isocratically with MeOH/H_2O (4:1, v/v) at a flow rate of 1 ml/min.

2.7. NMR measurement

For NMR analyses, a sample of ca. 700 μg β-apo-10′-carotenal was dissolved in 500 μl CD_2Cl_2. The NMR experiments were performed on a Bruker AVANCE II spectrometer operating at a ^1H resonance frequency of 400.13 MHz and equipped with a 5 mm ATM BBFO SmartProbe with a z-gradient coil and with pulse angles of 10 μs (^1H) and 10 μs (^{13}C), respectively. Bruker TOPSPIN software (version 3.0, patch level 3) was used to acquire and process the NMR data. The measurements were carried out at room temperature (298 K). For the 1D ^1H experiment, a standard one-pulse experiment (zg) was used with 32 transients, a spectral width of 12 ppm, a data size of 32 K points, a relaxation delay of 5 s, and an acquisition time of 3.41 s Unambiguous signal assignment of the ^1H resonances was performed based on 2D ^1H–^1H-COSY, ^1H–^{13}C-HSQC, and ^1H–^{13}C-HMBC experiments. For 2D ^1H–^1H-NOESY (Supplementary Fig. 12), the gradient-enhanced phase-sensitive NOESY experiment (noesygpphpp) was applied with a mixing time of 200 ms. 32 transients, a relaxation delay of 1 s, an acquisition time of 0.22 s, a spectral width of 11.5 ppm in both dimensions (f2, f1), 2048 and 256 acquired data points in f2 and f1 respectively were used. Data were processed by zero filling (to 1024) in f1 and by using shifted squared sine window functions in both dimensions prior to 2D Fourier transformation. For 2D ^1H–^1H-COSY the gradient-enhanced COSY experiment for magnitude mode of detection (*cosygpqf*), 32 scans, a relaxation delay of 1 s, an acquisition time of 0.43 s, a spectral width in both dimensions (f2, f1) of 12 ppm, 4096 and 256 acquired data points in f2 and f1 respectively were used. Data were processed by zero filling (to 1024) in f1 and by using unshifted squared sine window functions in both dimensions prior to 2D Fourier transformation. For 2D ^1H–^{13}C-HSQC, the gradient-enhanced HSQC experiment with carbon multiplicity editing and echo–antiecho acquisition mode (*hsqcedetgpsisp2.2*), 32 transients, a relaxation time of 1.5 s, an acquisition time of 0.21 s, spectral widths of 12 ppm and 190 ppm (in f2 and f1), with 2048 and 256 acquired data points respectively, were used. Data were processed by zero-filling (to 1024) and linear prediction in f1, and by using shifted squared sine window functions in both dimensions prior to Fourier transformation. For 2D ^1H–^{13}C-HMBC, the gradient-enhanced HMBC experiment with twofold low-pass J-filter to suppress one-bond correlations and echo-antiecho acquisition mode (*hmbcetgpl3nd*), 64 transients, a relaxation time of 1 s, an acquisition time of 0.21 s, spectral widths (in f2 and f1) of 12 ppm and 240 ppm with 2048 and 256 acquired data points respectively, were used. Data were processed by zero-filling (to 1024) and linear prediction in f1, and by using shifted sine window functions in both dimensions prior to Fourier transformation.

3. Results and discussion

To investigate the substrate specificity of AtCCD7 and PsCCD7, we expressed both enzymes as thioredoxin-fusion in BL21(DE3) *E. coli* cells, transformed with the plasmid pGro7 that encodes the groES-groEL-chaperone system, and performed in vitro assays with crude lysates according to [43]. Incubation with 9-*cis*-β-carotene led, as previously reported [24], to the supposed 9-*cis*-β-apo-10′-carotenal (Fig. 1, P1), besides β-ionone. Similarly, both enzymes cleaved the 9′,10′ double bond in 9-*cis*-zeaxanthin, leading to 9-*cis*-3-OH-β-apo-10′-carotenal (Fig. 1, P2) and 3-OH-β-ionone whose identities were confirmed by LC-MS (Supplementary Fig. 1). Due to the presence of two different ionone rings, lutein can occur as 9-*cis*- (the *cis* double bond is on the ε-ionone site) and 9′-*cis*-isomer (the *cis* double bond is on

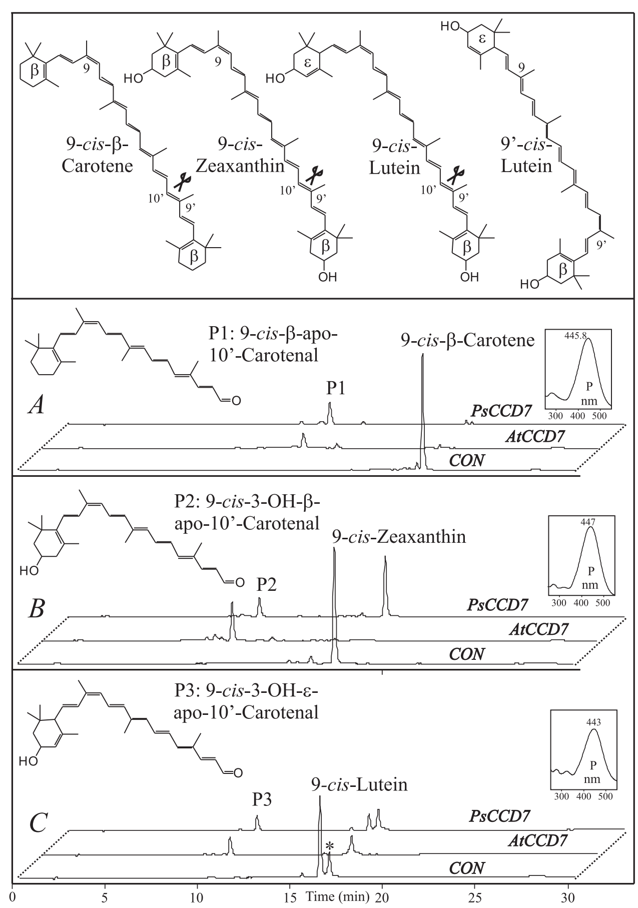

Fig. 1. HPLC analysis of AtCCD7 and PsCCD7 substrate specificity. Incubations with 9-*cis*-β-carotene (A) led to the 9-*cis*-β-apo-10′-carotenal (P1). Both enzymes converted also 9-*cis*-zeaxanthin into 9-*cis*-3-OH-β-apo-10′-carotenal (P2). Incubation of the two lutein isomers (9- and 9′-*cis*-lutein) unraveled the cleavage of the former into 9-*cis*-3-OH-ε-apo-10′-carotenal (P3), while the second substrate (peak *) remained unconverted. UV–Vis-spectra of the products are depicted in the insets. Above structures of the substrates tested showing the cleavage site at the 9′–10′ double bond.

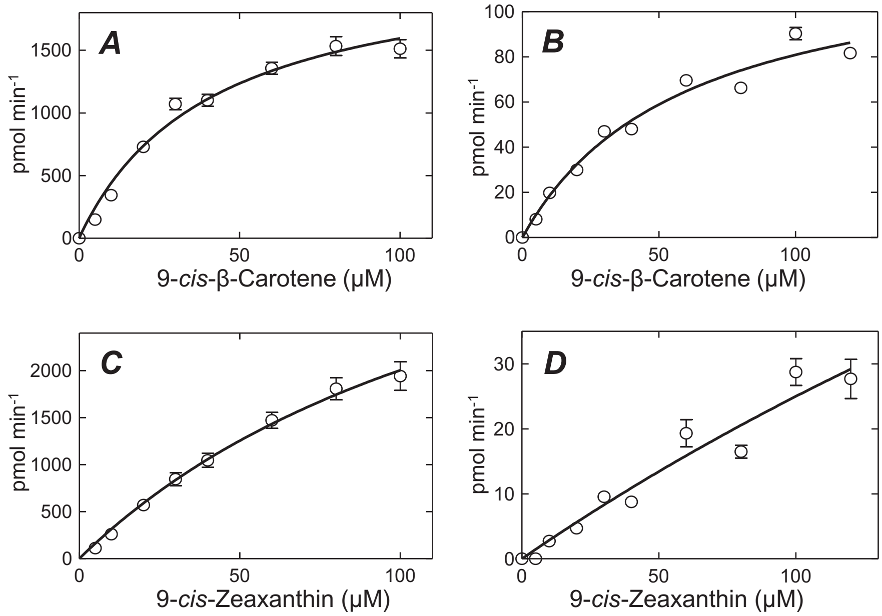

Fig. 2. Kinetics of AtCCD7 and PsCCD7. AtCCD7 and PsCCD7 were incubated with 9-*cis*-β-carotene (A, C) and 9-*cis*-zeaxanthin (B, D), respectively. Curves were fitted using the Michaelis–Menten equation (goodness of fit was determined as follows: $R2$ = 0.97 for A, 0.97 for B, 0.96 for C, and 0.91 for D). Curves represent the average of three technical replicates (±S.E.).

Table 1
V_{max} and K_m of AtCCD7 and PsCCD8. Values are deduced from Michaelis–Menten plots.

	AtCCD7		PsCCD7	
	9-*cis*-β-carotene	9-*cis*-zeaxanthin	9-*cis*-β-carotene	9-*cis*-zeaxanthin
V_{max} (pmol/min)	2251 ± 283	4989 ± 1873	129.2 ± 17.4	181.5*
K_m (μM)	41.1 ± 11.9	148.7 ± 81.7	59.6 ± 17.2	626.0*

* Values given are approximations. Due to the high K_m value, experiments with higher substrate concentrations would be needed, which are beyond the scale of feasibility.

the β-ionone site, peak * in Fig. 1C). As shown in Fig. 1, the two enzymes converted mainly the tentative 9-*cis*-lutein into an apocarotenal (Fig. 1, P3) with a lightly shorter retention time and lower absorption maximum than those of 9-*cis*-3-OH-β-apo-10′-carotenal. Both features together with the nature of the precursor suggest that this product (P3) is 9-*cis*-3-OH-ε-apo-10′-carotenal. In contrast, we did not observe significant conversion of 9′-*cis*-lutein, indicating that the presence of a β-ionone ring on the all-*trans*-configured moiety of the substrate is a prerequisite for the cleavage. We also tested the conversion of 9-*cis*/9′-*cis*-cryptoxathin and 9-*cis*-violaxanthin. Both enzymes did not show any detectable conversion of 9-*cis*-violaxanthin (Supplementary Fig. 2A), indicating that CCD7 activity does not interfere with ABA biosynthesis that utilizes 9-*cis*-violaxanthin/9′-*cis*-neoxanthin as precursor, while 9-*cis*- and 9′-*cis*-cryptoxanthin were converted. The latter result is consistent with the activity with 9-*cis*-β-carotene and -zeaxanthin, to 9-*cis*-β-apo-10′- or 9-*cis*-3-OH-β-apo-10′-carotenal, respectively (Supplementary Fig. 2B). Supporting the previously reported stereo-specificity observed with β-carotene-isomers, both enzymes did not show detectable conversion of all-*trans*-lutein, -zeaxanthin or cryptoxanthin (data not shown).

To address the question on the substrate preference, we determined the K_m and V_{max} values of both enzymes for the substrates 9-*cis*-β-carotene and -zeaxanthin (Fig. 2). As shown in Table 1, the two enzymes displayed large differences in their kinetic parameters. AtCCD7 showed much higher V_{max} values and also higher affinity towards both substrates, compared with PsCCD7. Both enzymes have higher affinity to 9-*cis*-β-carotene than to -zeaxanthin, but convert the latter with higher rates.

Table 2
^{1}H and ^{13}C NMR data of β-apo-10′-carotenal produced by AtCCD7. Experimental resonance assignments (ppm) and relevant NOE cross peaks observed in the 2D-NOESY experiment of β-apo-10′-carotenal dissolved in CD_2Cl_2.

	^{1}H	^{13}C	^{1}H–^{1}H-NOESY
1	–	34.1	
2	1.53 (2H, m)	39.5	
3	1.68 (2H, m)	19.1	
4	2.09 (2H, t)	32.9	
5	–	129.5	
6	–	138.1	
7	6.29 (1H, d)	129.0	H-19
8	6.74 (1H, d)	129.5	H-11, no NOE for H-10
9	–	135.8	
10	6.12 (1H, d)	128.8	H-12 and H-19 no NOE for H-8
11	6.92 (1H, t)	125.5	H-8
12	6.36 (1H, d)	135.6	H-10, no NOE for H-11
13	–		
14	6.33 (1H, d)	131.2	
15	6.94 (1H, m)	135.0	
16	1.08 (3H, s)	28.6	
17	1.08 (3H, s)	28.6	
18	1.79 (3H, s)	21.4	
19	2.03 (3H, s)	20.3	H-7 and H-10
20	2.04 (3H, s)	12.6	
10′	9.6 (1H, d)	193.4	
11′	6.20 (1H, dd)	126.9	
12′	7.23 (1H, d)	156.3	
13′	–	133.6	
14′	6.68 (1H, d)	128.2	
15′	6.68 (1H, m)	140.8	
20′	2.00 (3H, s)	12.3	

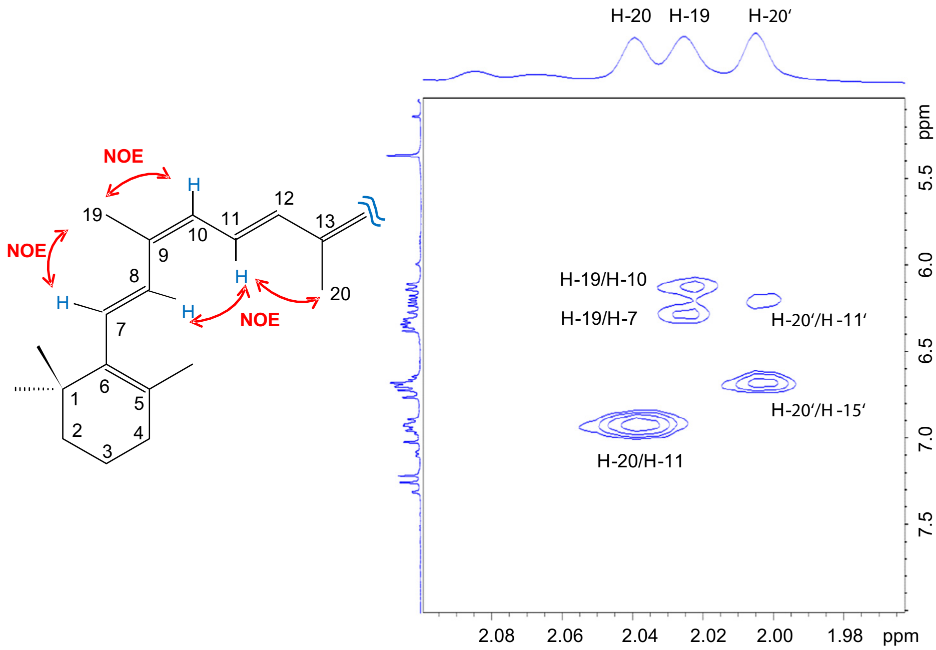

Fig. 3. Nuclear Overhauser effect spectroscopy plot. The structure of the apocarotenoid fragment shows the spatial proximity between the relevant H-protons of the 9-*cis*-structure. The stereochemistry was confirmed by the observed NOEs reported in Table 2 and shown on the right for an expansion of the 2D-NOESY spectrum revealing NOEs between methyl and olefinic proton signals.

The configuration of the apocarotenal produced by CCD7 is crucial for the investigation and mechanistic interpretation of the complex reactions sequence catalyzed by CCD8, yielding carlactone. Therefore, we determined the structure of the AtCCD7 product, using one- (1D, s. Supplementary Figs. 3–6) and two-dimensional (2D) NMR techniques. The ^{1}H and ^{13}C resonance assignments, which were based on the 2D HSQC, COSY and HMBC data (Supplementary Figs. 7–11), are summarized in Table 2. The 2D NOESY experiment allows detecting spatial proximity among protons and was thus most important for proving the 9-*cis*-configuration of the apocarotenal (see Fig. 3 and Supplementary Fig. 12). The most relevant observed NOEs are given in Table 2 and displayed for an expansion of the 2D-NOESY spectrum in Fig. 3. As is indicated by arrows in the apocarotenoid structure fragment (Fig. 3), the NOEs clearly supported the 9-*cis*-structure. This was proved by the existence of NOEs between the protons of the H-C19 methyl and the H-C10 olefinic groups, as well as between the H-C8 and H-C11 groups. Simultaneously, the absence of NOEs between the protons of the H-C19 methyl and the H-C11 olefinic groups on one hand, and the H-C8 and H-C10 groups on the other hand exclude the 9-*trans* structure.

Taken together, the two CCD7 are stereospecific enzymes that should be considered and designated nine-*cis*-carotenoid cleavage dioxygenases (NCCDs) and can be distinguished from NCEDs involved in ABA biosynthesis by the incapability of cleaving 9-*cis*-violaxanthin and by the different cleavage site. We are currently investigating whether CCD8 converts the hydroxylated apocarotenals produced from 9-*cis*-zeaxanthin and -lutein into carlactones with a hydroxylated β- or ε-ionone ring, which may be precursors of new strigolactones.

Acknowledgements

This work was supported by the German Research Foundation (DFG) Grant AL 892/1-4 and by the EU (METAPRO; FP7 KBBE-2009-3-1-01).

Appendix A. Supplementary data

Supplementary data associated with this article can be found, in the online version, at http://dx.doi.org/10.1016/j.febslet.2014.03.041.

References

[1] Xie, X., Yoneyama, K. and Yoneyama, K. (2010) The strigolactone story. Annu. Rev. Phytopathol. 48, 93–117.
[2] Seto, Y., Kameoka, H., Yamaguchi, S. and Kyozuka, J. (2012) Recent advances in strigolactone research: chemical and biological aspects. Plant Cell Physiol. 53 (11), 1843–1853.
[3] Ruyter-Spira, C., Al-Babili, S., van der Krol, S. and Bouwmeester, H. (2013) The biology of strigolactones. Trends Plant Sci. 18 (2), 72–83.
[4] Brewer, P.B., Koltai, H. and Beveridge, C.A. (2013) Diverse roles of strigolactones in plant development. Mol. Plant 6 (1), 18–28.
[5] de Saint Germain, A., Bonhomme, S., Boyer, F.D. and Rameau, C. (2013) Novel insights into strigolactone distribution and signalling. Curr. Opin. Plant Biol. 16 (5), 583–589.
[6] Waldie, T., McCulloch, H. and Leyser, O. (2014) Strigolactones and the control of plant development: Lessons from shoot branching. Plant J., http://dx.doi.org/10.1111/tpj.12488.
[7] Umehara, M., Hanada, A., Yoshida, S., Akiyama, K., Arite, T., Takeda-Kamiya, N., Magome, H., Kamiya, Y., Shirasu, K., Yoneyama, K., et al. (2008) Inhibition of shoot branching by new terpenoid plant hormones. Nature 455 (7210), 195–200.
[8] Gomez-Roldan, V., Fermas, S., Brewer, P.B., Puech-Pages, V., Dun, E.A., Pillot, J.P., Letisse, F., Matusova, R., Danoun, S., Portais, J.C., et al. (2008) Strigolactone inhibition of shoot branching. Nature 455 (7210), 189–194.
[9] Kapulnik, Y., Delaux, P.M., Resnick, N., Mayzlish-Gati, E., Wininger, S., Bhattacharya, C., Sejalon-Delmas, N., Combier, J.P., Becard, G., Belausov, E., et al. (2011) Strigolactones affect lateral root formation and root-hair elongation in Arabidopsis. Planta 233 (1), 209–216.
[10] Ruyter-Spira, C., Kohlen, W., Charnikhova, T., van Zeijl, A., van Bezouwen, L., de Ruijter, N., Cardoso, C., Lopez-Raez, J.A., Matusova, R., Bours, R., et al. (2011) Physiological effects of the synthetic strigolactone analog GR24 on root system architecture in Arabidopsis: another belowground role for strigolactones? Plant Physiol. 155 (2), 721–734.
[11] Rasmussen, A., Mason, M.G., De Cuyper, C., Brewer, P.B., Herold, S., Agusti, J., Geelen, D., Greb, T., Goormachtig, S., Beeckman, T., et al. (2012) Strigolactones suppress adventitious rooting in Arabidopsis and pea. Plant Physiol. 158 (4), 1976–1987.
[12] Snowden, K.C., Simkin, A.J., Janssen, B.J., Templeton, K.R., Loucas, H.M., Simons, J.L., Karunairetnam, S., Gleave, A.P., Clark, D.G. and Klee, H.J. (2005) The Decreased apical dominance1/Petunia hybrida CAROTENOID CLEAVAGE

DIOXYGENASE8 gene affects branch production and plays a role in leaf senescence, root growth, and flower development. Plant Cell 17 (3), 746–759.
[13] Agusti, J., Herold, S., Schwarz, M., Sanchez, P., Ljung, K., Dun, E.A., Brewer, P.B., Beveridge, C.A., Sieberer, T., Sehr, E.M., et al. (2011) Strigolactone signaling is required for auxin-dependent stimulation of secondary growth in plants. Proc. Natl. Acad. Sci. USA 108 (50), 20242–20247.
[14] Akiyama, K., Matsuzaki, K. and Hayashi, H. (2005) Plant sesquiterpenes induce hyphal branching in arbuscular mycorrhizal fungi. Nature 435 (7043), 824–827.
[15] Bouvier, F., Isner, J.C., Dogbo, O. and Camara, B. (2005) Oxidative tailoring of carotenoids: a prospect towards novel functions in plants. Trends Plant Sci. 10 (4), 187–194.
[16] Auldridge, M.E., McCarty, D.R. and Klee, H.J. (2006) Plant carotenoid cleavage oxygenases and their apocarotenoid products. Curr. Opin. Plant Biol. 9 (3), 315–321.
[17] Walter, M.H. and Strack, D. (2011) Carotenoids and their cleavage products: biosynthesis and functions. Nat. Prod. Rep. 28 (4), 663–692.
[18] Giuliano, G., Al-Babili, S. and Von Lintig, J. (2003) Carotenoid oxygenases: cleave it or leave it. Trends Plant Sci. 8 (4), 145–149.
[19] Medina, H.R., Cerda-Olmedo, E. and Al-Babili, S. (2011) Cleavage oxygenases for the biosynthesis of trisporoids and other apocarotenoids in Phycomyces. Mol. Microbiol. 82 (1), 199–208.
[20] Fraser, P.D. and Bramley, P.M. (2004) The biosynthesis and nutritional uses of carotenoids. Prog. Lipid Res. 43 (3), 228–265.
[21] DellaPenna, D. and Pogson, B.J. (2006) Vitamin synthesis in plants: tocopherols and carotenoids. Annu. Rev. Plant Biol. 57, 711–738.
[22] Cazzonelli, C.I. and Pogson, B.J. (2010) Source to sink: regulation of carotenoid biosynthesis in plants. Trends Plant Sci. 15 (5), 266–274.
[23] Moise, A.R., Al-Babili, S. and Wurtzel, E.T. (2013) Mechanistic aspects of carotenoid biosynthesis. Chem. Rev. 114 (1), 164–193.
[24] Alder, A., Jamil, M., Marzorati, M., Bruno, M., Vermathen, M., Bigler, P., Ghisla, S., Bouwmeester, H., Beyer, P. and Al-Babili, S. (2012) The path from beta-carotene to carlactone, a strigolactone-like plant hormone. Science 335 (6074), 1348–1351.
[25] Walter, M.H., Floss, D.S. and Strack, D. (2010) Apocarotenoids: hormones, mycorrhizal metabolites and aroma volatiles. Planta 232 (1), 1–17.
[26] Schmidt, H., Kurtzer, R., Eisenreich, W. and Schwab, W. (2006) The carotenase AtCCD1 from Arabidopsis thaliana is a dioxygenase. J. Biol. Chem. 281 (15), 9845–9851.
[27] Vogel, J.T., Tan, B.C., McCarty, D.R. and Klee, H.J. (2008) The carotenoid cleavage dioxygenase 1 enzyme has broad substrate specificity, cleaving multiple carotenoids at two different bond positions. J. Biol. Chem. 283 (17), 11364–11373.
[28] Ilg, A., Beyer, P. and Al-Babili, S. (2009) Characterization of the rice carotenoid cleavage dioxygenase 1 reveals a novel route for geranial biosynthesis. FEBS J. 276 (3), 736–747.
[29] Ilg, A., Yu, Q., Schaub, P., Beyer, P. and Al-Babili, S. (2010) Overexpression of the rice carotenoid cleavage dioxygenase 1 gene in Golden Rice endosperm suggests apocarotenoids as substrates in planta. Planta 232 (3), 691–699.
[30] Huang, F.C., Molnar, P. and Schwab, W. (2009) Cloning and functional characterization of carotenoid cleavage dioxygenase 4 genes. J. Exp. Bot. 60 (11), 3011–3022.
[31] Rubio, A., Rambla, J.L., Santaella, M., Gomez, M.D., Orzaez, D., Granell, A. and Gomez-Gomez, L. (2008) Cytosolic and plastoglobule-targeted carotenoid dioxygenases from Crocus sativus are both involved in beta-ionone release. J. Biol. Chem. 283 (36), 24816–24825.
[32] Auldridge, M.E., Block, A., Vogel, J.T., Dabney-Smith, C., Mila, I., Bouzayen, M., Magallanes-Lundback, M., DellaPenna, D., McCarty, D.R. and Klee, H.J. (2006) Characterization of three members of the Arabidopsis carotenoid cleavage dioxygenase family demonstrates the divergent roles of this multifunctional enzyme family. Plant J. 45 (6), 982–993.
[33] Gonzalez-Jorge, S., Ha, S.H., Magallanes-Lundback, M., Gilliland, L.U., Zhou, A., Lipka, A.E., Nguyen, Y.N., Angelovici, R., Lin, H., Cepela, J., et al. (2013) Carotenoid cleavage dioxygenase4 is a negative regulator of beta-carotene content in Arabidopsis seeds. Plant Cell 25 (12), 4812–4826.
[34] Ohmiya, A., Kishimoto, S., Aida, R., Yoshioka, S. and Sumitomo, K. (2006) Carotenoid cleavage dioxygenase (CmCCD4a) contributes to white color formation in chrysanthemum petals. Plant Physiol. 142 (3), 1193–1201.
[35] Campbell, R., Ducreux, L.J., Morris, W.L., Morris, J.A., Suttle, J.C., Ramsay, G., Bryan, G.J., Hedley, P.E. and Taylor, M.A. (2010) The metabolic and developmental roles of carotenoid cleavage dioxygenase4 from potato. Plant Physiol. 154 (2), 656–664.
[36] Brandi, F., Bar, E., Mourgues, F., Horvath, G., Turcsi, E., Giuliano, G., Liverani, A., Tartarini, S., Lewinsohn, E. and Rosati, C. (2011) Study of 'Redhaven' peach and its white-fleshed mutant suggests a key role of CCD4 carotenoid dioxygenase in carotenoid and norisoprenoid volatile metabolism. BMC Plant Biol. 11, 24.
[37] Rodrigo, M.J., Alquezar, B., Alos, E., Medina, V., Carmona, L., Bruno, M., Al-Babili, S. and Zacarias, L. (2013) A novel carotenoid cleavage activity involved in the biosynthesis of Citrus fruit-specific apocarotenoid pigments. J. Exp. Bot. 64 (14), 4461–4478.
[38] Ma, G., Zhang, L., Matsuta, A., Matsutani, K., Yamawaki, K., Yahata, M., Wahyudi, A., Motohashi, R. and Kato, M. (2013) Enzymatic formation of beta-citraurin from beta-cryptoxanthin and Zeaxanthin by carotenoid cleavage dioxygenase4 in the flavedo of citrus fruit. Plant Physiol. 163 (2), 682–695.
[39] Vogel, J.T., Walter, M.H., Giavalisco, P., Lytovchenko, A., Kohlen, W., Charnikhova, T., Simkin, A.J., Goulet, C., Strack, D., Bouwmeester, H.J., et al. (2010) SlCCD7 controls strigolactone biosynthesis, shoot branching and mycorrhiza-induced apocarotenoid formation in tomato. Plant J. 61 (2), 300–311.
[40] Schwartz, S.H., Qin, X. and Loewen, M.C. (2004) The biochemical characterization of two carotenoid cleavage enzymes from Arabidopsis indicates that a carotenoid-derived compound inhibits lateral branching. J. Biol. Chem. 279 (45), 46940–46945.
[41] Seto, Y., Sado, A., Asami, K., Hanada, A., Umehara, M., Akiyama, K. and Yamaguchi, S. (2014) Carlactone is an endogenous biosynthetic precursor for strigolactones. Proc. Natl. Acad. Sci. USA 111, 1640–1645.
[42] Schwartz, S.H., Qin, X. and Zeevaart, J.A. (2001) Characterization of a novel carotenoid cleavage dioxygenase from plants. J. Biol. Chem. 276 (27), 25208–25211.
[43] Alder, A., Holdermann, I., Beyer, P. and Al-Babili, S. (2008) Carotenoid oxygenases involved in plant branching catalyse a highly specific conserved apocarotenoid cleavage reaction. Biochem. J. 416 (2), 289–296.
[44] Barua, A.B. and Olson, J.A. (2000) B-carotene is converted primarily to retinoids in rats in vivo. J. Nutr. 130, 1996–2001.
[45] Tan, B.C., Joseph, L.M., Deng, W.T., Liu, L., Li, Q.-B., Cline, K. and McCarty, D.R. (2003) Molecular characterization of the Arabidopsis 9-cis epoxycarotenoid dioxygenase gene family. Plant J. 35, 44–56.